Comparison of two MPPT controls in a nano-grid

S. S. A. Ranaivoson[2,4], N. Le Saux[4], N. Saincy[4], E. J. R. Sambatra[1,2], T. D. Razafimahefa[2,3] , T. Andrianajaina[2,3]

[1]School of Industrial Engineering, Higher Institute of Technology of Antsiranana
[2]EDT Renewable Energies and Environment, University of Antsiranana
[3]Polytechnic School, University of Antsiranana
[4]Nanoé – Decentralized Electrification, Ambanja
sanda.ranaivo@gmail.com

Abstract— The aim of this article is to analyze the performance of maximum power generation in an electrical nanogrid using the MPPT technique. The components of an electric nanogrid are described, namely (i) a PV module, (ii) a buck converter and (iii) a MPPT controller. The Perturb and Observe " P&O " and Incrementing the Conductance " INC " commands were chosen to control a buck converter because of their simplicity of implementation. Simulations of these two commands under different atmospheric conditions, in an electrical nanogrid, are performed on the Matlab/Simulink © environment.

Keywords : Photovoltaic system, Electrical nanogrid, Buck converter, MPPT, P&O and INC.

I. INTRODUCTION

The Nanoé company Nanoéis deploying a new electrification model of electrification based on nano-electric grids in rural northern Madagascar. To meet the growing energy needs of households and to ensure the availability of energy in these nano-electric grids for their future connections, the use of a maximum power point tracking (MPPT) type solar charge controller is of great importance [1].

Among several MPPT commands to control this solar charge controller, the commands (i) disturbance and observation "P&O" and (ii) increase of the conductance "INC" are studied because of their simple implementation, since they only require current and voltage measurements of the photovoltaic module [2]–[5].

This paper gives an overview of the operation of an electrical nanogrid. Then, the Matlab/Simulink© environment is used to simulate the above two MPPT commands controlling a downward chopper under different atmospheric conditions. A discussion of the performance of these two commands follows, followed by a conclusion.

II. MODELE DU SYSTEME

An electrical nano-grid can be compared to a single photovoltaic solar array connecting 4 to 6 households, initially providing an electrical service limited to the essential domestic needs of the off-grid population (lighting, phone charging, multimedia, etc.)[1].

In this article, an electrical nano-grid is modeled, as shown in the following figure:

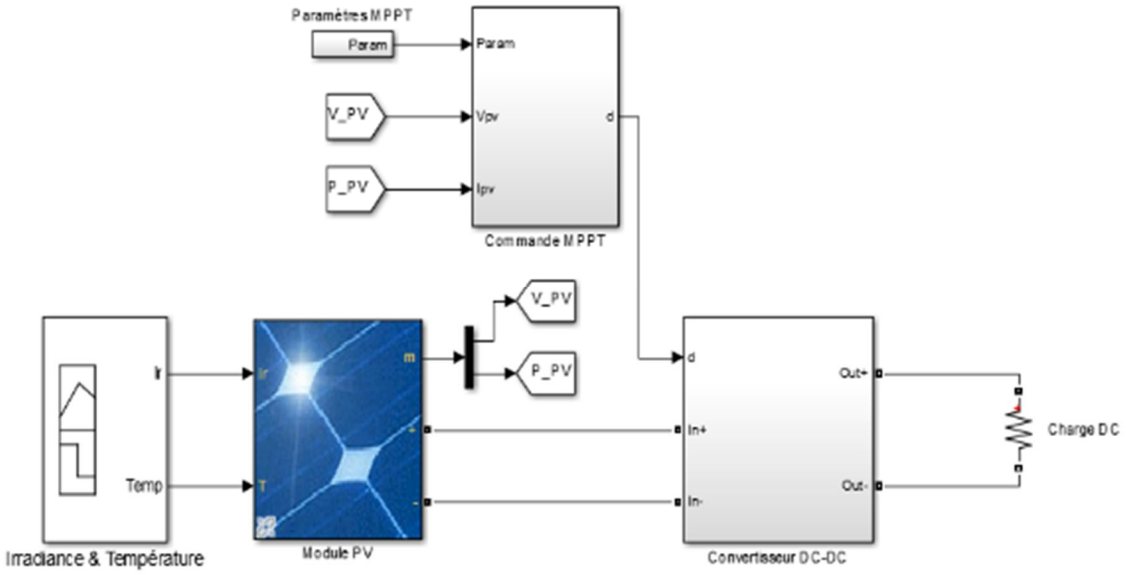

Fig.1 : Modélisation d'un nano-réseau électrique

It consists of (i) a PV module that generates electricity from an irradiation and a temperature, (ii) a direct-to-direct "DC-DC" converter that ensures matching of sourceand load , (iii) an MPPT command that controls the DC-DC converter via duty cycle, and (iv) and a DC load.

A. ***PV Module***

The PV module in Fig.1 is formed by the union of several PV cells, which can be considered as an ideal current source that provides a current proportional to irradiance and temperature. A PV cell can be modeled as follows [6], [7] :

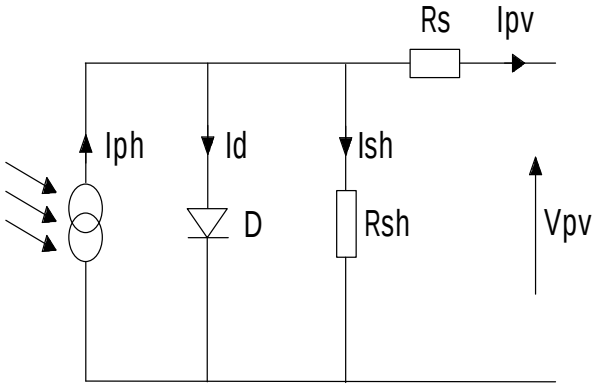

Fig.2 : Modèle à une diode d'une cellule photovoltaïque

The corresponding equations of the single diode model of a PV cell can be summarized as follows. :

$$I_{pv} = I_{ph} - I_d - I_{sh} \qquad \textbf{(1)}$$

- Photocurrent I_{ph} is expressed as a function of irradiance and temperature. :

$$I_{ph} = \frac{\phi}{\phi_{ref}}\left[I_{cc} + \mu_{Icc}\left(T - T_{ref}\right)\right] \qquad \textbf{(2)}$$

- It is assumed that the diode current is related to the temperature according to the expression :

$$I_d = I_{sat} * \left[\exp\left(\frac{V_{pv} + R_s I_{pv}}{n V_T} \right) - 1 \right] \quad \textbf{(3)}$$

- And the shunt current through the shunt resistor is equal to:

$$I_{sh} = \frac{V_{pv} + R_s I_{pv}}{R_{sh}} \quad \textbf{(4)}$$

With V_{pv} et I_{pv} represent the voltage and current of the PV cell, ϕ et ϕ_{ref} are real and reference irradiances $[W/m^2]$; T et T_{ref} are effective and reference temperatures $[°K]$; μ_{Icc} is the temperature coefficient of the short-circuit current I_{cc}; I_{sat} is the saturation current [A]; is the ideality factor of the junction ($1 < n < 3$) and the thermal voltage of the diode [V].

A-1) Current-voltage characteristic

The electrical parameters of the PV module used in this article are defined using the static current-voltage characteristic in Fig.3 [8].

The maximum voltage across the PV module, the so-called open circuit voltage $V_{CO} = 21{,}8\ [V]$ depends on the temperature of the PV cells. The value of the maximum current $I_{cc} = 6{,}18\ [A]$ if the PV module has a short circuit depends on the size of the PV module and the irradiance.
The single optimal point where the power is maximum (PPM) corresponds to the optimal voltage and amperage $V_{MPP} = 17{,}2\ [V]$ et $I_{MPP} = 5{,}8\ [A]$.

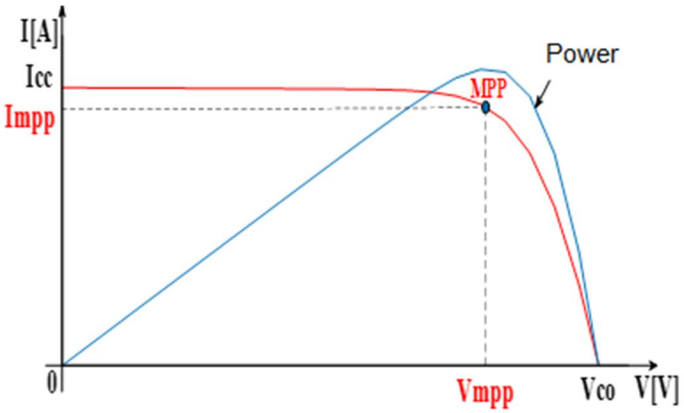

Fig.3 : Current I_{MPP}, Voltage V_{MPP} et power P_{MPP}optimals for PV 100 W on STC mode

B. Matching stage between a PV module and a load

In order to extract the maximum available power at the terminals of the PV module in **Fig.1** at any time and transfer it to the load, a static converter is usually used to act as an adapter between the source and the load[9]–[11] .

Nanogrids use a step-down chopper where the voltage of the load to be supplied DC must be less than or equal to the voltage of the PV module $V_{pv} \geq V_{charge}$ [9].

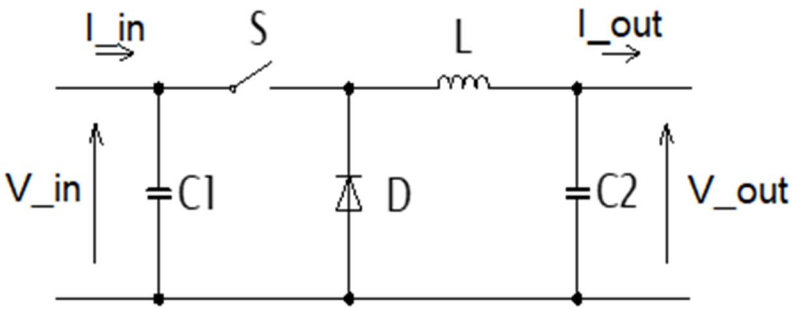

Fig.4 : Structure of a step-down chopper

A step-down chopper is a switching power supply that steps down the output voltage. Its operation can be divided into two phases, depending on the state of the switch S [10]:

- the switch is closed: the current supplied by the PV gradually charges the inductor L while t1 ∈ $\overline{0,\ dT}$, and the voltage at the output of the converter is defined by

$$V_{out} = V_{in} - V_L \qquad \textbf{(5)}.$$

- the switch is open during the switch is open during t2 ∈ $\overline{dT,\ T}$, the current crossing the inductor decreases and it opposes this time this reduction of the current

$$V_L = -V_{out} \qquad \textbf{(6)}.$$

The duty cycle is defined by the ratio between the ignition time of and the switching period:

$$d = \frac{t1}{T} \qquad \textbf{(7)}$$

So,

$$V_{out} = dV_{in} \qquad \textbf{(8)}$$

*C. **MPPT command***

Given the volatility of photovoltaic solar energy, the maximum power that a PV module can deliver and its optimal voltage and current are not known in advance [8]. Control laws are associated with the converter DC-DC that enable it to extract the maximum power from the PV module at any time [2], [3].

They are called MPPT (maximum power point tracking) and allow to control the converter DC-DC to ensure the best possible matching between the PV module and the load (Başoğlu, E. M. and Çakir, B., 2016). The most common of these commands are: (i) P&O, (ii) INC, open circuit voltage fraction (OCF) measurement, short circuit current fraction (FCC) measurement and control based on fuzzy logic (FL) [2].

In this article, we will talk about the first two, which are P&O and INC due to their extreme type [11], [12]These algorithms allow to follow the evolution of the power delivered by the PV module based on a perturbation of the duty cycle of the converter DC-DC, when all other commands are not applicable in terms of predictions [5].

C-1) P&O

The P&O method consists in perturbing the voltage V_{pv} and observing the effects on the output power of the PV module [2], [11], [12].

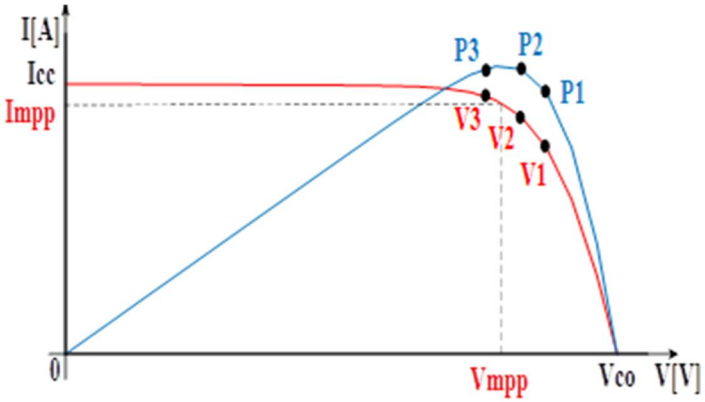

Fig. 5: Disruption of to reach the MPP, under STC conditions

At each cycle of Fig. 6, V_{pv} and I_{pv} are measured to calculate P_{pv} (k), which is compared with the previous power value P_{pv} (k-1).

If the output power increases, it is adjusted in the same direction as in the previous cycle. Otherwise, it is adjusted in the opposite direction than in the previous cycle. When the MPP (Maximum Power Point) is reached, it oscillates around the optimal voltage. This oscillation results in a loss of power that increases with the step size of the disturbance. However, a large step size allows the P&O algorithm to respond to sudden changes in operating conditions.

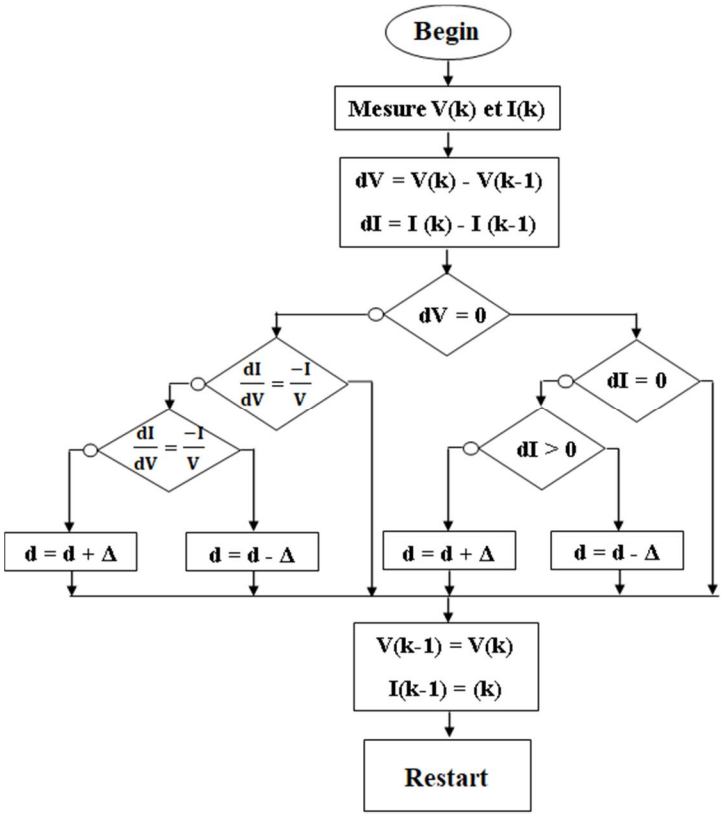

Fig.6 : P&O Algorithme

C-2) Conductance increment

This method is based on the calculation of the ratio of the derivatives of power and voltage

$$\frac{dP}{dV} \qquad \textbf{(9)}$$

to reach the maximum power point [2], [11], [12].

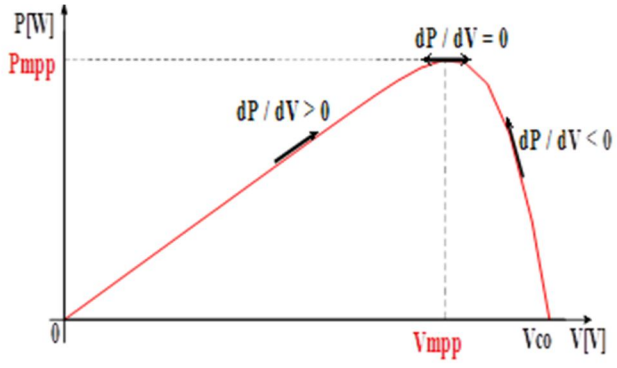

Fig. 7: MPP tracking by increasing the conductance

In the above figure, the ratio dP/dV is greater than zero to the left of the MPP, less than zero to the right of the MPP, and zero when equal to zero.

Knowing that the derivative of the product compared to the tension gives the relation :

$$\frac{dP}{dV} = \frac{d(V*I)}{dV} = I + V\frac{dI}{dV} \qquad \textbf{(10)}$$

Which mean :

$$\frac{dP}{dV} = 0 \text{ équivaut à } \frac{dI}{dV} = -\frac{I}{V} \qquad \textbf{(11)}$$

$$\frac{dP}{dV} > 0 \text{ équivaut à } \frac{dI}{dV} > -\frac{I}{V} \qquad \textbf{(12)}$$

$$\frac{dP}{dV} < 0 \text{ équivaut à } \frac{dI}{dV} < -\frac{I}{V} \qquad \textbf{(13)}$$

In **Fig.6**, the required incremental changes and by comparing the last measured values for and with the values measured in the previous cycle:

$$dV = V(k) - V(k-1) \qquad \textbf{(14)}$$

$$dI = I(k) - I(k-1) \qquad \textbf{(15)}$$

Thus, if relation (11) is true, the MPP is reached and no change in voltage *V(k)* is required. If relation (11) is false, the voltage *V(k)* is adjusted accordingly, depending on whether *V(k)* is higher (13) or lower (12) than V_{mpp}. Unlike P&O, INC stabilizes at the optimal voltage V_{mpp} once the point of maximum power MPP is reached. However, reaching this point during sudden fluctuations in operating conditions depends on the value of the increment step Δ.

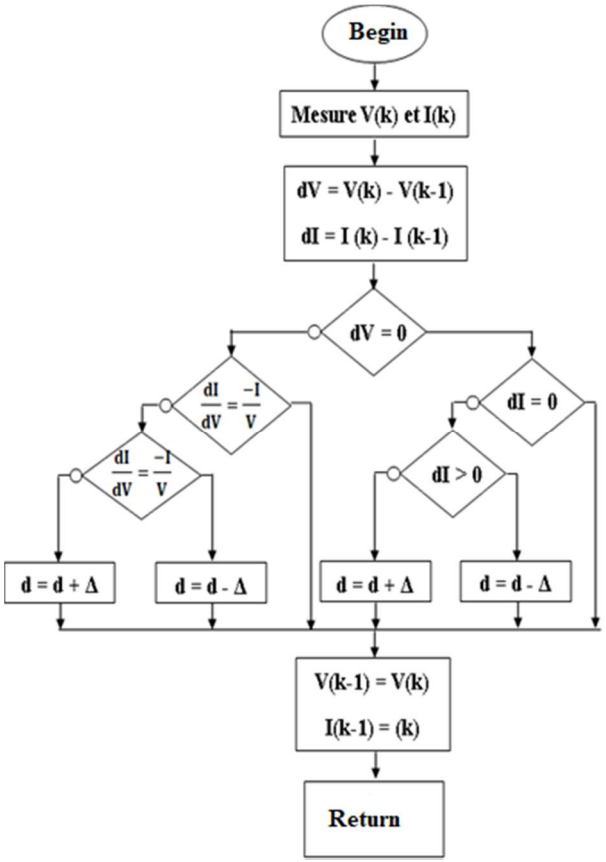

Fig. 8 : INC Algorithme

III. SIMULATIONS

A. Simulation results

A-1) STC Conditions

The PV module is exposed to an irradiance of 1000 W/m^2 and a temperature of 25°C. The Fig.7 and Fig.9 correspond to the predefined values in Fig.3 for the properties of the PV module in the STC state.

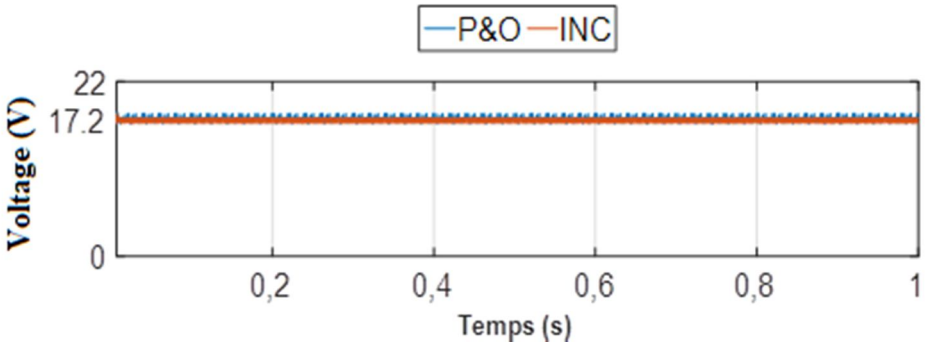

Fig. 9: Optimal PV voltage in STC

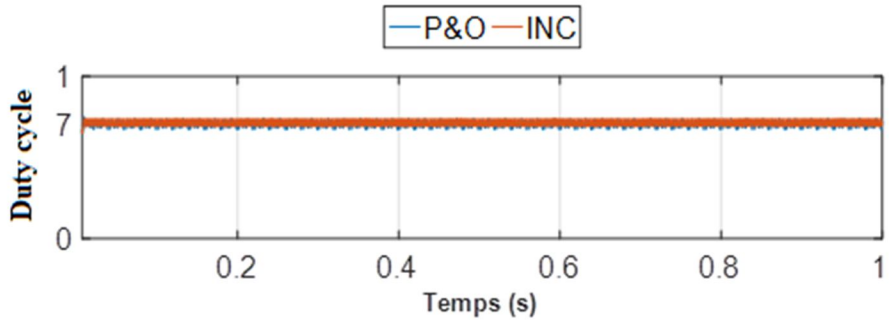

Fig. 10: Duty cycle of the step-down chopper

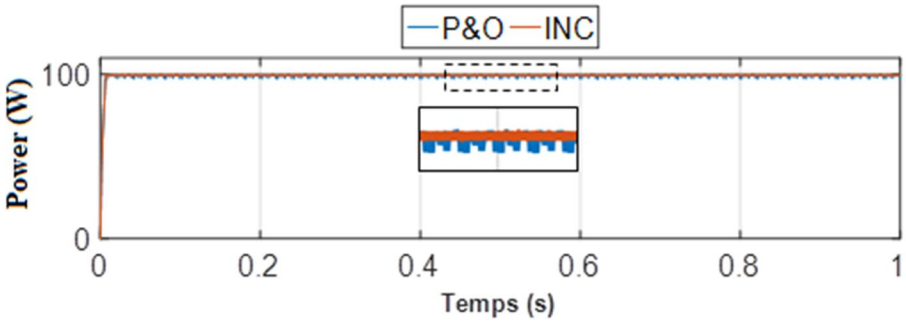

Fig. 11: Optimal PV power in STC

A-2) Case of irradiance variation

The PV system is simulated with a fixed temperature of 25°C and a variable irradiance with a step of 100 W/m2 (100 W/m2 - 500 W/m2). The following figures illustrate the evolution of the PV system characteristics as a function of the irradiance evolution at a fixed temperature.

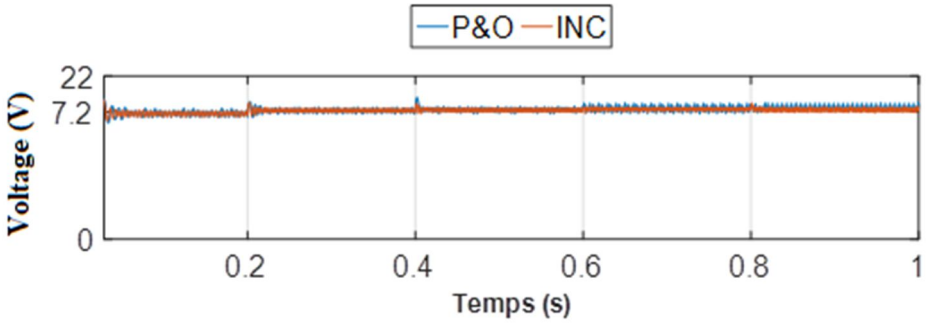

Fig. 12: Optimal PV voltage with varying irradiance.

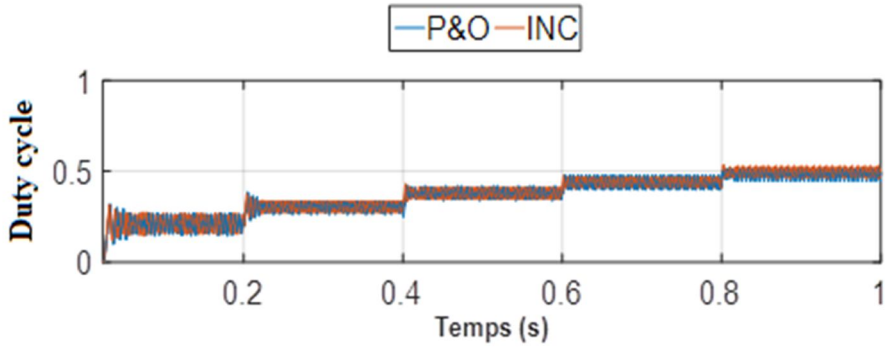

Fig. 13: Operating cycle of the step-down chopper

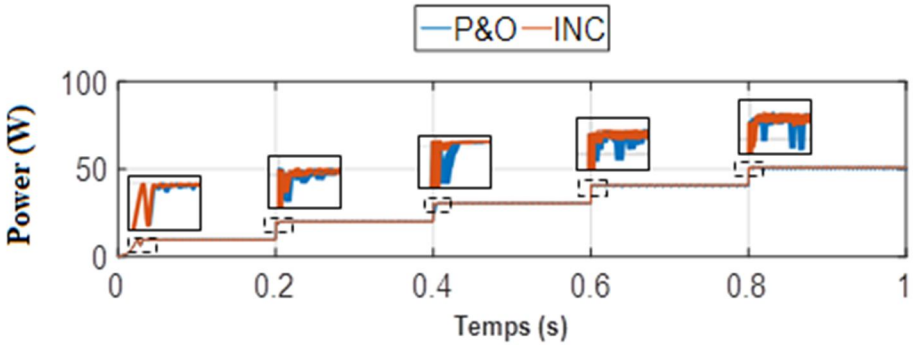

Fig. 14: Optimal PV power with irradiation variations

A-3) Case of temperature variations

The third simulation is performed with a fixed irradiance of 1000 W/m^2 and a variable temperature with a step of 5°C (25°C - 45°C). The following figures illustrate the evolution of the PV system characteristics according to the evolution of the temperature with a fixed irradiance.

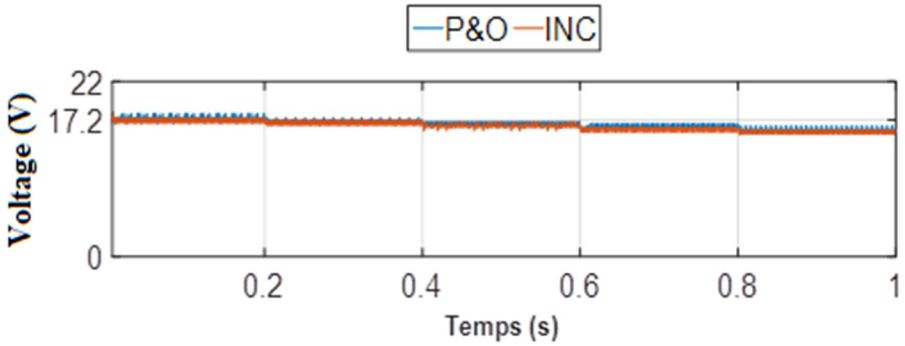

Fig. 15: Optimal PV voltage with temperature variation

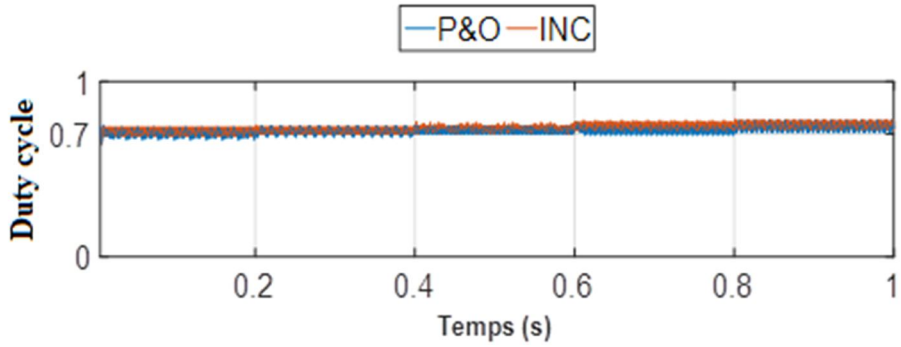

Fig. 16: Operating cycle of the step-down chopper.

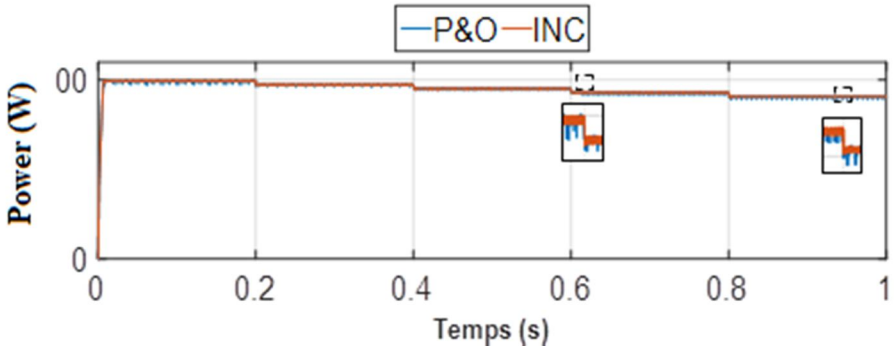

Fig. 17: Optimal PV power at temperature variation

A-4) Case of irradiance and temperature variation

The last simulation is performed with a variable irradiance with a step of 100 W/m2 (100 W/m2 - 500 W/m2) and a variable temperature with a step of 5°C (25°C - 45°C).

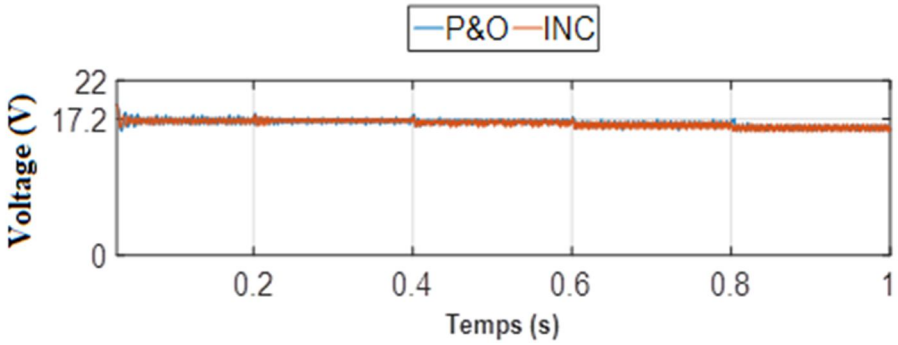

Fig. 18: Optimal PV voltage with a double variation of temperature and irradiance.

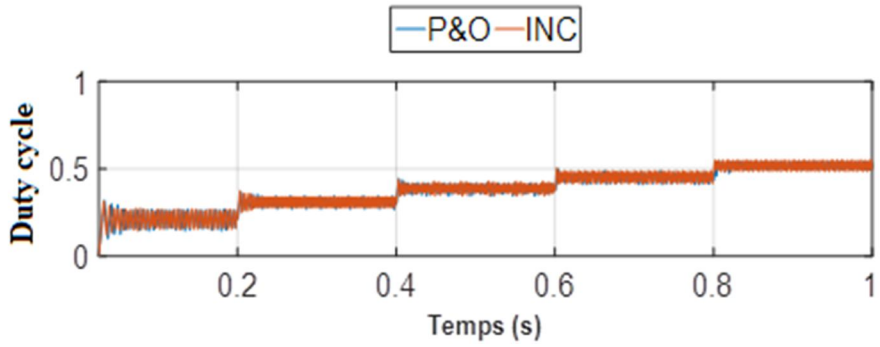

Fig. 19: Step-down chopper duty cycle.

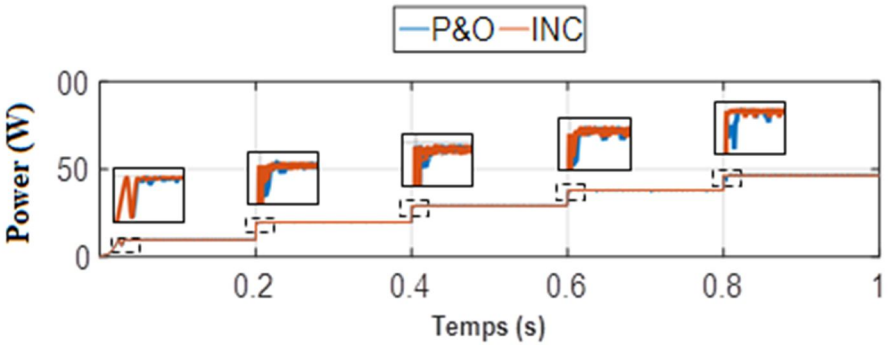

Fig. 20: Optimal PV power at a double variation of temperature and irradiance.

*B. **Discussion***

In the four different simulation conditions, (i) STC condition, (ii) constant temperature and variable irradiance, (iii) variable temperature and constant irradiance, and (iv) variable temperature and irradiance, the voltage, duty cycle, and power have the same pace with both P&O and INC commands to reach the optimal value of PV.

In the first simulation under STC conditions, the optimal voltage and power defined in Fig.3 are achieved with the two commands. The duty cycle of the buck chopper stabilizes at 0.72 with both commands.

Unlike the INC command, fluctuations around the optimal values are observed with the P&O command.

In the second simulation with a temperature of 25°C, the optimal power is proportional to the change in irradiance, which directly affects the current generated by the PV according to equation (2). However, the PV voltage is approximately stable and oscillates around the MPP voltage.

Compared with the INC control, the P&O control has some anomalies in the stable state and shifts the operating point to the wrong direction after a sudden change of irradiance.

In the third simulation with irradiance of 1000 W/m^2, the temperature variation affects the voltage generated by the PV system. This temperature variation is inversely proportional to the variation of the power supplied by the PV, and the duty cycle approaches unity (according to equation (8)) as the optimal voltage tends to the value of the output voltage.

The P&O controller has difficulty in following the sudden fluctuations, and the oscillations around the optimal power are always present even under stable conditions.

From the last simulation, the disadvantage of the P&O control compared to the INC control can be deduced in the case of sudden variations of irradiation and temperature.

The power curves in Fig.12 and Fig.18 look the same. However, the PV system provides less power in the last simulation than in the second simulation.

IV. CONCLUSION

This work aims to generate the maximum power in an electrical nano-grid using a powerful and easy to implement MPPT controller. The main elements of a photovoltaic system, namely (i) the PV module, (ii) the down-chopper, and (iii) the P&O and INC controls have been described. Then, in order to analyze and compare the performance of these two controllers, simulations were performed under different irradiation and temperature conditions using the Matlab/Simulink© environment.
The simulation results show that the INC command gives better results than the P&O command, both under stable conditions and under variations in atmospheric conditions. Moreover, the power generated by the PV module is proportional to the change in irradiance, which is not the case when the temperature is changed. Note that irradiance has a larger effect on the power generated by a PV module than temperature, as shown in the last three simulations and equation (2).
This paper leads to the development of a prototype step-down chopper controlled by the command INC to have a high performance MPPT solar charge controller in a nano-grid.

ACKNOWLEDGMENTS

We thank Nanoé very much, especially the two referents who allowed this study to be carried out. I am quoting N. Le Saux and N. Saincy.

REFERENCES

[1] C. Murphy *et al.*, « Electrification Futures Study Supply-Side Scenarios Report Figure Data », National Renewable Energy Laboratory - Data (NREL-DATA), Golden, CO (United States); National Renewable Energy Lab. (NREL), Golden, CO (United States), FY18 AOP 2.4.0.3, janv. 2021. doi: 10.7799/1762488.

[2] S. Motahhir, A. El Hammoumi, et A. El Ghzizal, « Photovoltaic system with quantitative comparative between an improved MPPT and existing INC and P&O methods under fast varying of solar irradiation », *Energy Reports*, vol. 4, p. 341□350, nov. 2018, doi: 10.1016/j.egyr.2018.04.003.

[3] A. K. Pandey, V. Singh, et S. Jain, « Chapter eleven - Study and comparative analysis of perturb and observe (P&O) and fuzzy logic based PV-MPPT algorithms », in *Applications of AI and IOT in Renewable Energy*, R. N. Shaw, A. Ghosh, S. Mekhilef, et V. E. Balas, Éd. Academic Press, 2022, p. 193□209. doi: 10.1016/B978-0-323-91699-8.00011-5.

[4] R. S. Pal et V. Mukherjee, « Metaheuristic based comparative MPPT methods for photovoltaic technology under partial shading condition », *Energy*, vol. 212, p. 118592, déc. 2020, doi: 10.1016/j.energy.2020.118592.

[5] A. F. Sagonda et K. A. Folly, « A comparative study between deterministic and two meta-heuristic algorithms for solar PV MPPT control under partial shading conditions », *Systems and Soft Computing*, vol. 4, p. 200040, déc. 2022, doi: 10.1016/j.sasc.2022.200040.

[6] T. Andrianajaina, E. J. R. Sambatra, C. Bernard Andrianirina, T. David Razafimahefa, et N. Heraud, « PV fault detection using the least squares method », in *2016 International Conference and Exposition on Electrical and Power Engineering (EPE)*, oct. 2016, p. 846□851. doi: 10.1109/ICEPE.2016.7781456.

[7] T. ANDRIANAJAINA, D. T. RAZAFIMAHEFA, N. HERAUD, et E. J. R. SAMBATRA, « ANOVA fault detection method in photovoltaic system », in *2020 7th International Conference on Control, Decision and Information Technologies (CoDIT)*, juin 2020, vol. 1, p. 37□41. doi: 10.1109/CoDIT49905.2020.9263843.

[8] L. Bun, « Détection et localisation de défauts pour un système PV », phdthesis, Université de Grenoble, 2011. Consulté le: 27 septembre 2022. [En ligne]. Disponible sur: https://tel.archives-ouvertes.fr/tel-00647189

[9] M. Boillot, A. Doulet, et N. Saincy, « Electrification latérale : Vers un nouveau modèle d'électrification pour l'Afrique. Paris : Fondation Tuck ». Fondation Tuck, 1 mai 2018. Consulté le: 27 septembre 2022. [En ligne]. Disponible sur: https://www.fondation-tuck.fr/sites/fondation-tuck.fr/files/telechargements/documents/MISSIONS/RECHERCHE/Future%20of%20Energy/2017%20-%20ALGORUS-LE%20-%20Report.pdf

[10] P. V. Nandankar, P. P. Bedekar, et P. V. Dhawas, « Efficient DC-DC converter with optimized switching control: A comprehensive review », *Sustainable Energy Technologies and Assessments*, vol. 48, p. 101670, déc. 2021, doi: 10.1016/j.seta.2021.101670.

[11] S. Jagtap et A. Khandekar, « Implementation of Combined System between Perturb & Observe and Incremental Conductance Technique for MPPT in PV System », in *2021 2nd Global Conference for Advancement in Technology (GCAT)*, oct. 2021, p. 1□6. doi: 10.1109/GCAT52182.2021.9587457.

[12] H. Yatimi, Y. Ouberri, R. Marah, E. Aroudam, et S. Chahid, « Design of an Incremental Conductance Maximum power point tracking Controller based on Automation PLC for PV Applications », in *2021 International Conference on Electrical, Communication, and Computer Engineering (ICECCE)*, juin 2021, p. 1□6. doi: 10.1109/ICECCE52056.2021.9514239.